# The Comparison Reflectometer

D. L. HOLLWAY, SENIOR MEMBER, IEEE

*Abstract*—**The comparison reflectometer is an instrument designed to locate and measure the characteristics of reflections in waveguide and transmission-line systems: it is particularly suitable for measuring small reflections in precise microwave measuring instruments up to one meter in length.**

**It consists of a reflectometer in which the returning waves are combined with an accurately known reference wave and a measure of the total reflection coefficient is recorded automatically on punched paper tape at a number of preset frequencies covering a particular waveband. From sets of readings taken without, and with, the test component connected, a computer calculates and plots the distribution of reflections as a function of distance and prints out their magnitudes and phases.**

**The reflection coefficients of individual discontinuities are also plotted by the computer as a function of frequency on Smith charts.**

**Under suitable conditions point reflections may be located in *X*-band waveguide within a few tenths of a millimeter and measured with an accuracy of ±3 percent in magnitude and ±5° in phase angle.**

**The method compensates for imperfections in the reflectometer and so reduces the background level of spurious reflections to less than 0.00006.**

## Introduction

During the development of a waveguide bridge intended for the precise measurement of attenuation, a phase shifter was required having a negligible change in attenuation with phase and very low reflections over the whole waveband. The most promising of several designs tried consisted of a "concertina" constructed from flexible waveguide, for which the change in attenuation per half-wave change in length was below 0.002 dB. However, progress was hampered by the fact that this, and several other components of the bridge, had reflection coefficients of 0.01–0.02 and these varied rapidly with frequency.

It was the need to locate and remove these small reflections which led to the development of the comparison reflectometer described in the following sections.

When microwave components, such as those used in the attenuation bridge, were measured on an ordinary reflectometer [1], it was often noticed that the magnitude of the reflection coefficient showed a sinusoidal variation with frequency, usually superimposed on a complex wave. These sinusoids show up most clearly when the component contains two discrete reflections, slightly different in magnitude, and spaced an appreciable distance apart. The number of peaks in the plot is equal to the difference between the numbers of half-waves occurring between the reflections at the top, and at the bottom, of the frequency band.

To determine the spacing, a protractor was constructed having a set of curves which could be matched with the peaks of the plot. Unexpectedly it was found possible to measure the spacing quite accurately—within a millimeter or two—and this stimulated interest in further development.

Manuscript received March 14, 1966; revised November 29, 1966.
The author is with the Division of Applied Physics, National Standards Laboratory, C.S.I.R.O., Sydney, Australia.

## The Comparison Reflectometer

As many components, although mismatched, showed little evidence of sinusoidal variations in their reflection coefficients, the first improvement needed was to ensure that each reflection contributed a sine component related to its distance from a known reference plane. This was done by placing between the directional coupler and the component being measured a standard, or reference, reflection larger in magnitude than the total reflection from the component. In this way reflections from the test component are compared with a known wave from the reference and for this reason the instrument has been named a "comparison reflectometer."

With the exception of the reference reflection the microwave equipment consists largely of a conventional reflectometer. However, the method of operation is different and enables a comparison reflectometer to determine the moduli and phase angles of individual reflections as a function of distance along a component under test, whereas an ordinary reflectometer cannot.

In its present form the comparison reflectometer consists of the equipment shown in Fig. 1. Microwave energy, square-wave modulated at 1 kHz, is transmitted from the backward-wave sweep generator through the directional couplers and is partially reflected by the reference reflection at the right-hand end of the waveguide. The forward and reflected waves produce 1 kHz signals at the crystal detectors and these are compared in the ratiometer. The dc voltage at the output of the ratiometer is read by the digital voltmeter and the result is punched on paper tape by the serializer and punch. The sequence controller provides a set of 76 preset voltages which control the frequencies of the backward-wave oscillator. Because the oscillator drifts, provision is made for rapidly checking and setting the frequencies by feeding energy into a resonant cavity consisting of a length of *X*-band waveguide two meters long. It is more convenient to work at frequencies equally spaced in wave number $\nu$, equal to the reciprocal of the wavelength in waveguide, rather than frequency, and the values chosen correspond to 68, 69, 70, and so on through to 143 half-waves in the two-meter length. For setting the control potentials these resonances may be displayed by frequency modulating the oscillator over a range of ±3 MHz and they may be selected manually in sequence or in any order.[1]

[1] An alternative method, of phase-locking these frequencies to harmonics of a crystal oscillator, has been adopted recently. Full details of the comparison reflectometer will be given in a report now in preparation and available on request.

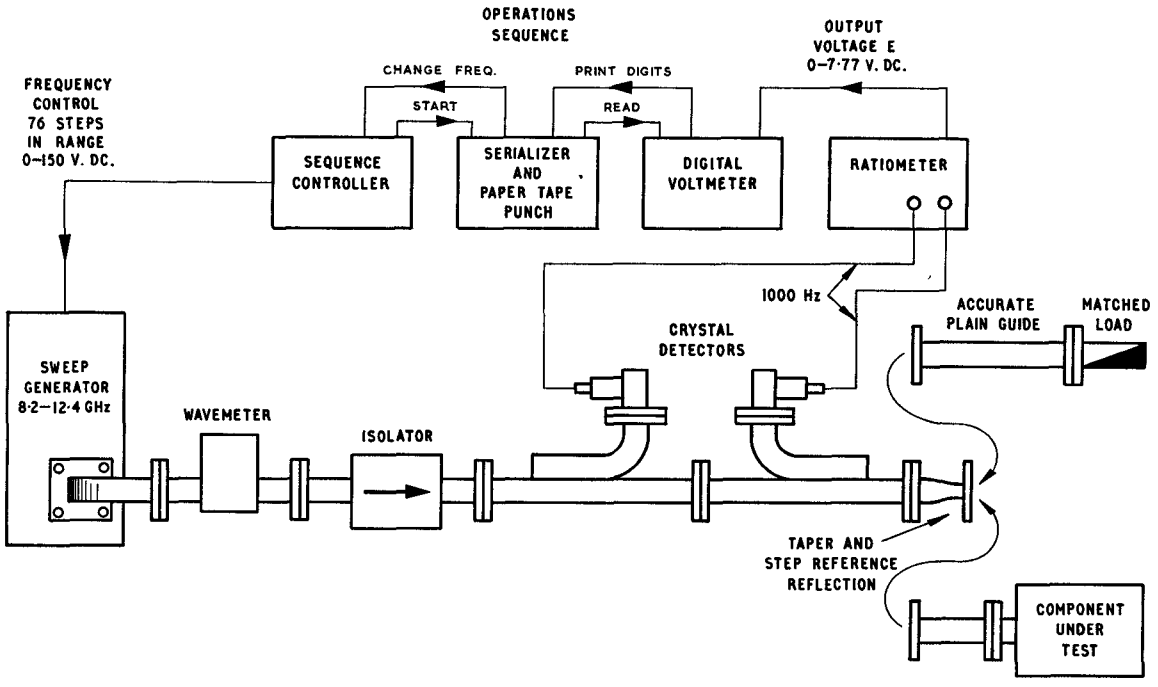


Fig. 1. A block diagram of the comparison reflectometer used for locating and measuring reflections in $X$-band waveguide.

Whenever a component is measured by the comparison reflectometer, two sets of voltage readings are recorded, a "reference" set and a "measurement" set. For the reference set, a length of accurate plain waveguide is attached to the reference reflection, Fig. 1, and terminated by a matched load. The sequence controller then steps the oscillator through the 76 preset frequencies, recording the ratiometer output voltage at each. The plain waveguide and load are then removed and the measurement set of readings is recorded with the component under test connected to the reference reflection, usually by a short length of plain guide. If the component has output ports, these are fitted with matching loads.

The data tape is then read by a digital computer together with a program which computes and prints the in-phase and quadrature components, moduli and phase angles of the individual reflections as a function of distance along the component under test. They are also plotted on suitable scales by a plotter attached to the computer. From these plots the operator may select regions of particular interest. The corresponding distances are then fed in with other programs which instruct the computer to prepare, from the original data, Smith charts showing the variation of the local reflection coefficient with frequency at a given number of planes spaced at some prescribed distance apart.

The method of producing these plots, their accuracy and examples of their use are given in the following sections.

## The Reflection Coefficient as a Function of Distance

Consider a waveguide system in which a component having a single reflection $|\Gamma_1| e^{j\theta}$ is connected to a reference reflection having the scattering coefficients shown in Fig. 2, located at the reference plane. The reflection coefficient of the combination may be written,

$$\frac{b_1}{a_1} = \frac{S_{22}(1 - S_{33}\Gamma_1) + S_{32}\Gamma_1 S_{23}}{1 - S_{33}\Gamma_1} = \frac{S_{22} - \Gamma_1(S_{22}S_{33} - S_{32}S_{23})}{1 - S_{33}\Gamma_1}. \quad (1)$$

In general, the reflection being measured will be located at some distance $l_1$ from the reference plane, so that the value of $\Gamma_1$ measured at this plane will be,

$$\Gamma_1 = |\Gamma_1| e^{j(\theta - 2\beta l_1)}.$$

Both the theory and the computation are simplified, and the accuracy of the results is improved if a reference reflection is used having a coefficient which is essentially constant in magnitude and phase throughout the frequency band at a stationary reference plane. A design which has been found superior to others in this respect consists of a symmetrical $E$-plane taper, having only small reflections, followed by a sudden step back to the full guide height. As the taper is on the generator side of the step, its length is not included in the distance $l_1$.

For the present purpose[2] this step reflection, shown in Fig. 3(a), may be represented by a lossless transformer having a turns ratio $N$, set in the guide at the reference plane as in Fig. 3(b). If $\Gamma_r$ is the reflection coefficient of this reference as seen from the generator side,

$$\Gamma_r = S_{22} = (N^2 - 1)/(N^2 + 1), \quad (2)$$

$$S_{33} = (1 - N^2)/(1 + N^2), \quad (3)$$

[2] The small correction required for step capacitance is introduced later.

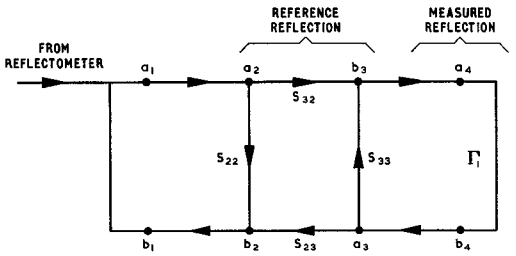


Fig. 2. Flowgraph showing the generator, reference reflection, and a single-point reflection.

and

$$S_{32} = S_{23} = 2N/(1 + N^2). \tag{4}$$

From this point on $\Gamma_r$ will be assumed to have zero phase angle and it will be written without a modulus sign, the subscript $r$ serving as a reminder that it is both the reference reflection and also apparently resistive.

The total reflection coefficient at the reference plane is, therefore,

$$\Gamma = \frac{b_1}{a_1} = \frac{\Gamma_r(1 + \Gamma_r\Gamma_1) + S_{32}S_{23}\Gamma_1}{1 + \Gamma_r\Gamma_1}, \tag{5}$$

and since

$$\begin{aligned} S_{32}S_{23} &= 1 - \Gamma_r^2, \\ \Gamma &= (\Gamma_r + \Gamma_1)/(1 + \Gamma_r\Gamma_1) \\ &= \frac{\Gamma_r + |\Gamma_1| e^{j(\theta - 2\beta l)}}{1 + \Gamma_r |\Gamma_1| e^{j(\theta - 2\beta l)}}. \end{aligned} \tag{6}$$

To rearrange (6) into a form suitable for computation, let

$$c = |\Gamma_1| \cos(\theta - 2\beta l)$$

and

$$s = |\Gamma_1| \sin(\theta - 2\beta l).$$

Thus,

$$\Gamma = (\Gamma_r + c + js)/(1 + \Gamma_r(c + js)) \tag{7}$$

$$= \frac{\Gamma_r(1 + |\Gamma_1|^2) + c(1 + \Gamma_r^2) + js(1 - \Gamma_r^2)}{1 + 2\Gamma_r c + \Gamma_r^2 |\Gamma_1|^2}. \tag{8}$$

Part of the return wave passes through a directional coupler and produces a dc voltage which is independent of the phase of $\Gamma$. If a crystal detector is used, the output may be made proportional to $|\Gamma|^2$. From (8),

$$|\Gamma|^2 = \frac{\Gamma_r^2(1 + |\Gamma_1|^2)^2 + 2c\Gamma_r(1 + |\Gamma_1|^2)(1 + \Gamma_r^2) + c^2(1 + \Gamma_r^2)^2 + s^2(1 - \Gamma_r^2)^2}{(1 + 2c\Gamma_r + \Gamma_r^2 |\Gamma_1|^2)^2}. \tag{9}$$

As we are concerned chiefly with small reflections, terms such as $\Gamma_r^3|\Gamma_1|^3$ are small compared with unity; $8\times10^{-6}$ for $\Gamma_r=0.2$ and $|\Gamma_1|=0.1$. Ignoring these, and terms containing $\cos 2(\theta-2\beta l)$, the denominator may be written,

$$= 1/(1 - 4c\Gamma_r + 4\Gamma_r^2 |\Gamma_1|^2). \tag{10}$$

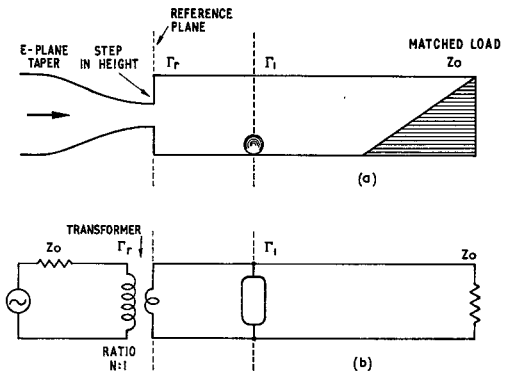


Fig. 3. (a) The taper and $E$-plane-step reference reflection and (b) its transmission-line equivalent circuit.

With these approximations,

$$|\Gamma|^2 \cong \Gamma_r^2 + |\Gamma_1|^2 - 2\Gamma_r^2|\Gamma_1|^2 + 2\Gamma_r|\Gamma_1| \cdot \cos(\theta - 2\beta l)(1 - \Gamma_r^2 - |\Gamma_1|^2 + \Gamma_r^2|\Gamma_1|^2). \tag{11}$$

In order to compute $|\Gamma_1|\cos(\theta-2\beta l)$, (11) may be rearranged to

$$|\Gamma_1| \cos(\theta - 2\beta l) = G(\nu) - (\Gamma_r^2 + |\Gamma_1|^2 - 2\Gamma_r^2|\Gamma_1|^2)/2\Gamma_r k \tag{12}$$

where

$$G(\nu) = |\Gamma|^2/2\Gamma_r k \tag{13}$$

and

$$k = 1 - \Gamma_r^2 - |\Gamma_1|^2 + \Gamma_r^2|\Gamma_1|^2.$$

$G(\nu)$ is a function of the wavenumber to be determined from the readings of the digital voltmeter as described in the next section. $k$ is a correction term near unity; for the moment let $k=1-\Gamma_r^2$.

So far only one reflection has been considered in addition to the reference. In general, the components being measured will contain a number of reflections, $\Gamma_1, \Gamma_2, \cdots, \Gamma_n, \cdots$ at distances $l_1, l_2, \cdots, l_n, \cdots$ and these must be computed from the data $G(\nu)$.

Assuming that interactions between these reflections may be neglected and that the right-hand term of (12) does not vary with $\nu$, by superposition,

$$G(\nu) = \sum_{n=1}^{\infty} |\Gamma_n| \cos(\theta_n - 4\pi l_n \nu),$$

which may be written as the Fourier series,

$$G(\nu) = \sum_{n=1}^{\infty} [a_n \cos(4\pi n l' \nu) + b_n \sin(4\pi n l' \nu)], \tag{14}$$

where $l'$ is a constant "unit length," $n$ is an integer and

$$l_n = nl'. \tag{15}$$

The component reflections are found by taking the finite Fourier transforms[3]

$$a_n = \frac{1}{\nu'} \int_{\nu_1}^{\nu_2} G(\nu) \cos (n\pi\nu/\nu')d\nu \tag{16}$$

$$b_n = \frac{1}{\nu'} \int_{\nu_1}^{\nu_2} G(\nu) \sin (n\pi\nu/\nu')d\nu \tag{17}$$

where $2\nu'$ is the range between the wavenumber limits $\nu_2$ and $\nu_1$ in which $G(\nu)$ is known and $l'$, the unit length, is related to the wavenumber range by,

$$l' = 1/4\nu'. \tag{18}$$

From (16) and (17),

$$|\Gamma_n| \cos\theta_n = a_n \tag{19}$$

$$|\Gamma_n| \sin\theta_n = b_n \tag{20}$$

$$|\Gamma_n| = \sqrt{a_n^2 + b_n^2} \tag{21}$$

and

$$\theta_n = \tan^{-1}(b_n/a_n). \tag{22}$$

The first value of $|\Gamma_n|$ may be used to find a closer approximation to $k$ and corrected values from (19), (20), and (21).

In order to obtain smooth curves, particularly near the peaks of individual reflections, $a_n$ and $b_n$ must be computed at small intervals of distance. At present an interval of 0.25 cm is used but this is increased to 0.5 cm in regions where the output is very small. These intervals are much smaller than the unit distance $l'$ but if nonintegral values of $n$ are used, small spurious fluctuations appear in the computer output. To remove this "noise" $\nu'$ is varied slightly for each integration so that (15) and (18) are always satisfied by the largest possible integral value of $n$.

The distance $l$ cannot be smaller than $l'$, corresponding to $n=1$, the lowest integral value. The maximum value of $l$ is one-half the length of the waveguide cavity used in setting the frequencies at which $G(\nu)$ is measured. At present $l_{(\max)} = 100$ cm.

It is interesting to note that although the phase angle of the total reflection $\Gamma$ was lost when the reflected signals were rectified by the detector crystal, both the magnitude and phase of individual reflections may be computed from the transforms.

Figure 4 shows a typical example of a plot of reflection coefficient as a function of distance computed by the use of (16) through (22). In this test a step reflection, similar in design to the reference reflection, was placed 30 cm from the reference and terminated by a matched load. The magnitude and phase (not shown) are correct at the position of the peak. The factors controlling the breadth of the curve, or "line width," and the height of the sidelobes, are discussed in a later section.

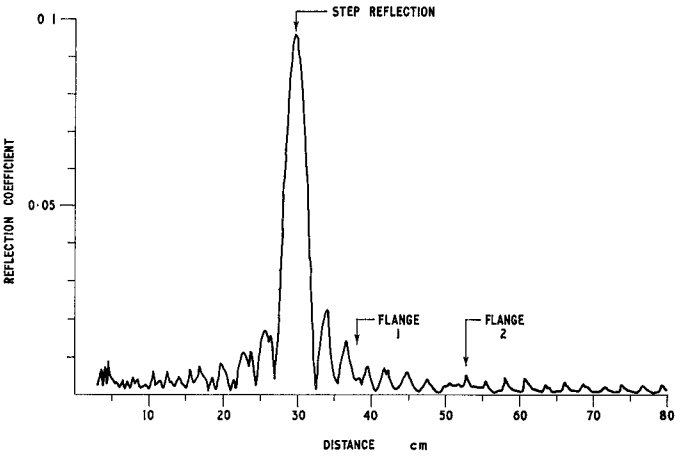


Fig. 4. The reflection coefficient modulus as a function of distance along a waveguide containing a step, of nominal value 0.1, placed 30 cm from the reference plane.

## The Method of Measuring $G(\nu)$

Rectified voltages from the forward and reverse crystals, shown in Fig. 1, enter the ratiometer where they are amplified and a voltage is produced which is related to the total reflection coefficient $|\Gamma|$, but is largely independent of the generator output.

If $r$ is the ratio of the rectified voltages,

$$r \propto |\Gamma|^x.$$

By choosing a particular temperature, crystal shunting resistor and range of operating power, the exponent $x$ may be made equal to 2.0 with an error of less than 1 percent in $\sqrt{r}$. The output voltage $E$ from the ratiometer is directly proportional to an angle of conduction $\gamma$ which appears only within the instrument[4] and $\tan\gamma \propto r$. The angle of conduction $\gamma_{\max}$, corresponding to the output voltage at full scale $E_{\max}$, is found by measuring the output $E$ for different values of $r$ and choosing the value of $\gamma_{\max}$ which best fits the tangent relationship.

In using the comparison reflectometer, two readings are recorded for each value of $\nu$, one with the reference reflection terminated by a matched load and the second after connecting the components to be tested. If the first reading, for $\Gamma_r$ only, results in a conduction angle $\gamma_r$ and a ratiometer output voltage $E_r$, and the corresponding values for the second reading are $\Gamma$, $\gamma$, and $E$, we have,

$$|\Gamma|^2 = \Gamma_r^2 \tan\gamma/\tan\gamma_r$$
$$= \Gamma_r^2 \tan (E\gamma_{\max}/E_{\max})/\tan (E_r\gamma_{\max}/E_{\max}). \tag{23}$$

Therefore, from (13),

$$G(\nu) = \Gamma_r \tan (E\gamma_{\max}/E_{\max})/2k \tan (E_r\gamma_{\max}/E_{\max}). \tag{24}$$

[3] $a_n$ and $b_n$ in (16) and (17) are not related to the symbols used in Fig. 2.

[4] This relationship between $E$ and $r$ applies to the particular ratiometer used, a Hewlett-Packard Model 416 A.

Before recording the reference set of readings, the ratiometer gain should be set so that $E_r$ is roughly 0.35 times $E_{max}$ as this allows the greatest excursion in $\Gamma$ for a given value of $\Gamma_r$. The gain may be increased if the test component has only small reflections. If $E_{max}$ is exceeded at any time, the test must be repeated using a larger reference reflection.

As an alternative, more general method of relating the output voltage $E$ with the microwave input, a table of measured values could be stored in the computer and interpolated.

### The Cancellation of Instrumental Reflections

All reflectometers suffer from small imperfections such as a lack of perfect directivity in the directional couplers and discontinuities in the couplings and elsewhere. In addition, the two crystal detectors usually have somewhat different frequency responses and these can cause changes in the output resembling those from reflections. The coupling coefficients of the directional couplers also vary slightly with frequency.

In the comparison reflectometer all measurements are made by comparison with a single known standard, the reference reflection, and all these instrumental defects are largely cancelled out.

This may be seen most easily by considering a test component having no internal reflections. When the reference readings are taken, all the instrumental defects show up as a variation in $E_r$ with frequency. However, the test readings $E$ will be equal to $E_r$ at every frequency and from (24) it will be seen that $G(\nu)$ is constant; thus $a_n = b_n = 0$ in (16) and (17), the instrumental reflections having been cancelled completely.

When the test component includes reflections, a high degree of cancellation is still obtained. The instrumental defects correspond to a pattern of reflections spaced at different distances from the reference. Because these contribute to both sets of readings, only a small residue can appear in $G(\nu)$, and then only when a reflection in the test component $\Gamma_t$ falls within a line width or so of an instrumental reflection $\Gamma_i$. In the worst case, when the two coincide in position and phase, it may be shown that,

$$|\Gamma_t|_{(\text{measured})} = |\Gamma_t|_{(\text{true})}(1 - |\Gamma_i|\,|\Gamma_t|). \quad (25)$$

As $\Gamma_i$ is small this error usually may be neglected.

A far more serious error would result from any defect which changed the apparent value of the reference reflection. In its method of operation the comparison reflectometer bears a family resemblance to a potentiometer, with the reference reflection corresponding to the standard cell. Thus any change in the apparent value of either cell or reference would result in a proportional error in the measurement. A similar result would be caused by any drift in the sensitivity of the measuring system between the two sets of readings. However, this would be indicated by incomplete cancellation of the instrumental reflections. The degree of cancellation now obtained is shown in Fig. 9 and discussed in a later section.

### The Elimination of the Sidelobes

Although plots of reflection coefficient as a function of distance, similar to that shown in Fig. 4, correctly give the locations and magnitudes of the major reflections, it was found during the course of the work that these plots have the disadvantage that sidelobes of a large reflection decay comparatively slowly with distance and tend to mask smaller reflections even when spaced several line widths away. This difficulty led to a different method for computing the transforms, which virtually removes the sidelobes and so reduces the masked region to a minimum.

To describe this method we shall first find an expression for the shape of a typical curve, or line, computed from (16) and (17) in the region of a typical point reflection $\Gamma_n$ at a distance $l_n$, equal to $n$ times the unit distance $l'$, from the reference plane. For simplicity assume that the phase angle at the reflection is zero and,

$$G(\nu) = |\Gamma_n| \cos(\pi n\nu/\nu'). \quad (26)$$

Let the normalized line profile be given by $y$, a function of $l\,(=xl')$ and let $y=1$ at the line center where $x=n$.[5]

Equations (16) and (17) may be written,

$$a_x + jb_x = \frac{1}{\nu'}\int_{\nu_1}^{\nu_2} G(\nu)\epsilon^{j\pi x\nu/\nu'}d\nu \quad (27)$$

therefore,

$$y = \frac{1}{\nu'}\int_{\nu_1}^{\nu_2} \cos(\pi n\nu/\nu')\epsilon^{j\pi x\nu/\nu'}d\nu$$

$$= \frac{1}{2\nu'}\int_{\nu_1}^{\nu_2}\left\{\epsilon^{-j\pi(n-x)\nu/\nu'} + \epsilon^{j\pi(n-x)\nu/\nu'}\right\}d\nu \quad (28)$$

and if $\nu_c = (\nu_1+\nu_2)/2$,

$$y = \frac{\sin\pi(n-x)}{\pi(n-x)}\epsilon^{-j\pi(n-x)\nu_c/\nu'} + \frac{\sin\pi(n+x)}{\pi(n+x)}\epsilon^{-j\pi(n+x)\nu_c/\nu'}. \quad (29)$$

As $n$ and $x$ are usually comparatively large ($x=11$ at $l=27$ cm) the right-hand term is small. Also, the fact that the wavenumber range is not centered on zero, i.e., $\nu_c \neq 0$ results only in a change in phase. As we are not now concerned with the phase, $\nu_c$ may be set at zero and (28) rewritten,

$$|y| = \left|\frac{1}{2\nu'}\int_{-\infty}^{\infty} P(\nu)\epsilon^{-j\pi(n-x)\nu/\nu'}d\nu\right| \quad (30)$$

where $P(\nu)=1$ between $\nu_1$ and $\nu_2$ and is zero elsewhere.

Thus

$$|y| = \frac{\sin\pi(n-x)}{\pi(n-x)} = \operatorname{sinc}\pi(n-x). \quad (31)$$

[5] The method used to compute (16) and (17) results in smooth curves and not points separated by $l'$. For examining the line shape these curves can be approximated by allowing $x$ to take nonintegral values.

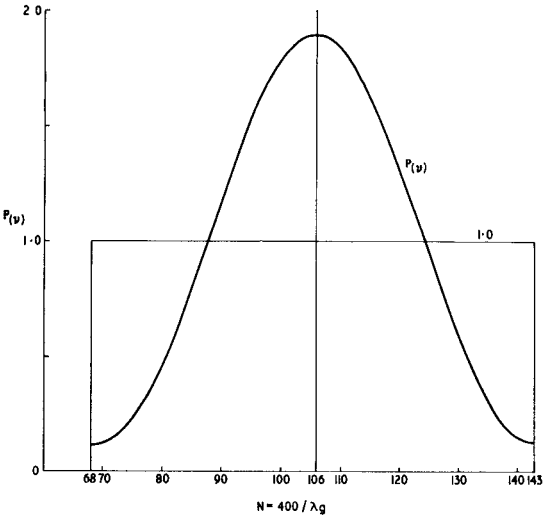


Fig. 5. The shaping function $P(\nu)$ used to eliminate sidelobes. $N$ is the number of half-wavelengths in a test waveguide 200-cm long.

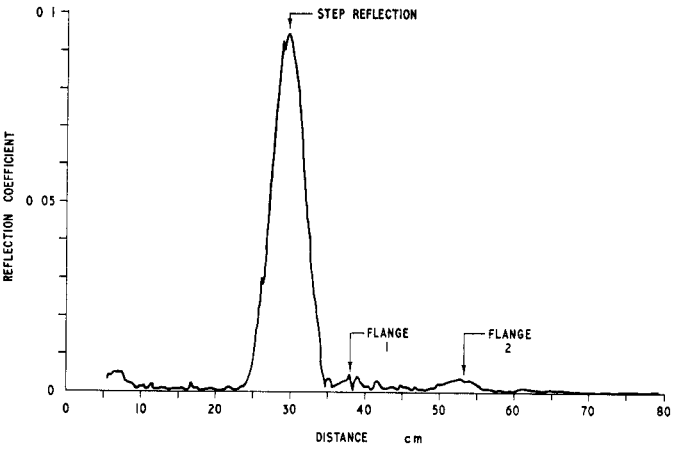


Fig. 6. A plot of $|\Gamma| - l$ showing the advantage of eliminating the sidelobes. The same data was used as in Fig. 4 but small reflections at $l = 38$ cm and at 53 cm, which were masked by sidelobe noise in Fig. 4, stand out clearly against the reduced background.

From (31) the line shape $y$ may be recognized as the Fourier transform of a rectangular pulse, of unit height and width $2\nu'$, which has a central lobe and a succession of diminishing sidelobes familiar in the spectra of pulses.

The problem of reducing these sidelobes frequently occurs in other fields; for example, in communications various pulse shapes have been proposed and used. The present problem is to find a shape having a transform which becomes negligible as close to the center of the line as possible and remains negligible further out.

Willis and Sinha [2] devised several suitable functions and the choice between them depends upon the maximum permissible level of the sidelobes. Of course, each reduction in this level must be paid for by an increase in width of the main lobe and a good compromise is provided by the shaping function shown in Fig. 5, from Willis and Sinha's equation (13). This may be rewritten in terms of the present variables,

$$P(\nu) = 1 - 0.889 \cos \frac{2\pi(\nu - \nu_1)}{(\nu_2 - \nu_1)} + 0.0112 \cos \frac{4\pi(\nu - \nu_1)}{(\nu_2 - \nu_1)} \cdot \quad (32)$$

When $G(\nu)$ is replaced by the product $G(\nu) \cdot P(\nu)$ in (16) and (17), the main lobe of a reflection expands to about the same width as the three central lobes of the unmodified line but beyond this point falls in amplitude to below 0.6 percent of the peak, instead of its former value 13 percent. This reduces spurious fluctuations in the region of a point reflection $\Gamma = 0.1$ from 0.013 to less than 0.0006 and so removes almost all the sidelobe "noise" from the trace.

Figure 6 shows the reflection from a step $\Gamma \simeq 0.1$ computed in this way. The experimental data are identical with those used in Fig. 4 and the magnitude and phase is in agreement, but a comparison between the figures shows the effect of the shaping function in removing the sidelobes. The small reflections at 38 cm and 53 cm are difficult to identify in Fig. 4 but stand out clearly in Fig. 6.

## The Reflection Coefficient as a Function of Both Frequency and Distance

The curves of reflection coefficient as a function of distance, described in the previous sections, are used chiefly for locating individual reflections and estimating their characteristics. The typical plots shown in Figs. 4 and 6 have been computed from data extending over the whole wavenumber band, as this provides the narrowest possible lines. The line at 30 cm in Fig. 4 is approximately one unit length ($l'$) wide at the half-power point and $l' = \frac{1}{4}\nu'$ where $2\nu'$ is the wavenumber range.

Once the distribution of reflections is known, however, it is often desirable to examine a particular reflection in more detail and to measure its coefficient as a function of frequency while keeping the distance from the reference plane constant. The distance required is usually that corresponding to the peak of the selected reflection, but as this often falls between calculated points, a second computer program has been written which calculates the magnitudes and phases of the reflection coefficients at a number of frequencies equally spaced in wavenumber in the band 8.3–12.6 GHz and automatically plots the points in a form suitable for tracing directly onto a Smith chart. The computer chooses the largest suitable scale from among the five standard printed Smith chart forms in use at the Laboratory, having reflection coefficient ranges of 0.027, 0.11, 0.22, 0.40, and 1.0. The center frequencies are marked on the plot at intervals of 0.5 GHz. Similar curves are then drawn for a specified number of planes separated by a small distance, such as 0.5 mm or 1 mm, towards and away from the generator. From these curves the peak of a particular reflection line usually may be located accurately by interpolation and the curves give a clear picture of changes in the complex reflection coefficient in this region.

Several measurements have been made to test the accuracy of this method in practice. Reflections which were primarily resistive, inductive and capacitive were measured both by the comparison reflectometer and by an accurate slotted-guide

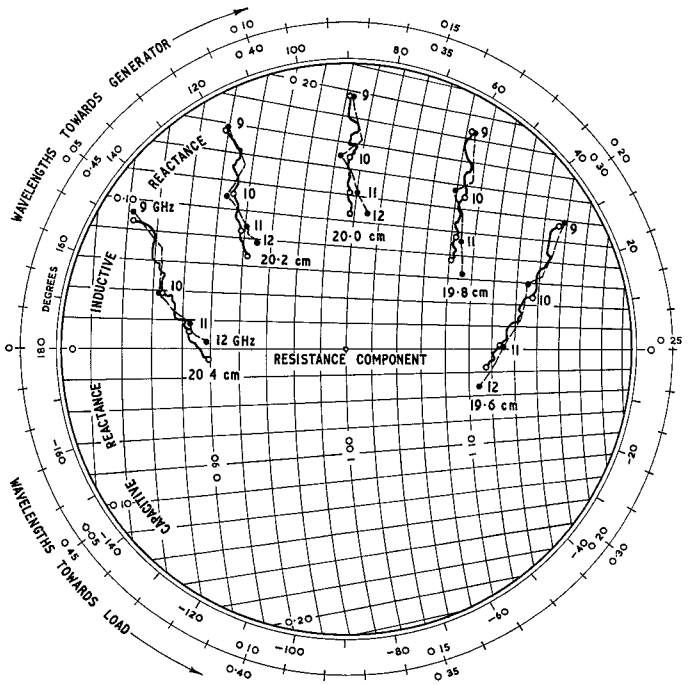


Fig. 7. The reflection coefficient of an inductive iris shown as a function of frequency at different distances. The full lines, plotted by the comparison reflectometer, agree closely with the standing-wave impedance measurements, shown dotted.

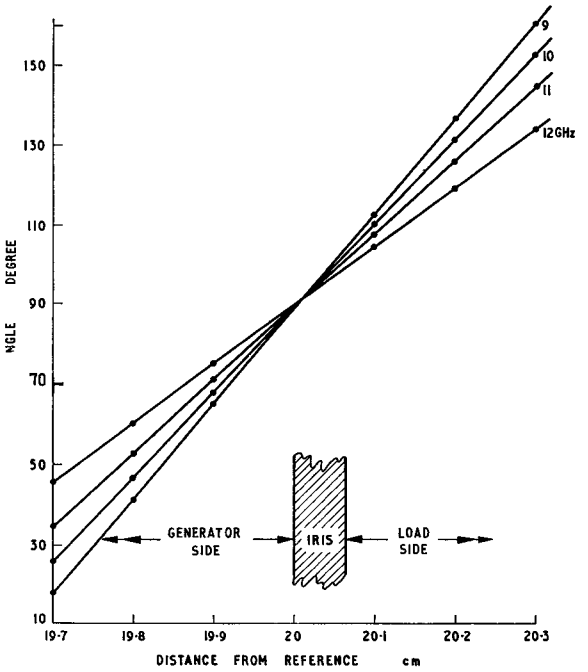


Fig. 8. The variation of phase angle with frequency shown at planes close to the center of a thin inductive iris, plotted from measurements by the comparison reflectometer. There is agreement between the four frequency lines at the point of minimum phase change.

standing-wave impedance meter. It was seen from the first test that, although the reflection coefficients agreed in magnitude within 2 percent, the phase angles of small reflections measured by the slotted guide showed much more scatter than those of the comparison reflectometer. The slotted-guide technique was then improved by phase-locking the klystron to a crystal oscillator and by taking several sets of readings at points near the minimum of the standing wave. This reduced the scatter roughly to that of the reflectometer but the experimental procedure was very exacting and time-consuming, even though the calculations and plotting were done by the computer. By contrast, the comparison reflectometer produced results of equal or better accuracy and its operation was almost completely automatic.

Figure 7 is a portion of a Smith chart showing a typical comparison between measurements by the two methods of a thin inductive iris. The full lines pass through 27 points computed from measurements by the reflectometer for overlapping wavenumber ranges and the slotted-line measurements, shown dotted, were made at 7 frequencies, using a calibrated attenuator to determine the standing-wave ratios.

In Fig. 8 the phase angles from the reflectometer measurements in Fig. 7 have been plotted against distance, on an expanded scale, to discover how closely points from different parts of the frequency band agree in defining the plane of minimum phase change with frequency. The intersection is approximately 0.1 mm from the metal surface and at this point all four lines intersect at a phase angle of 92°. In this way isolated, discrete reflections usually may be located to within a few tenths of a millimeter.

Plots similar to Fig. 8 have been used to examine the *E*-plane step reflections used as the reference standards. The reflection coefficient of the step has been computed from an expression given by Marcuvitz [3] which includes the effect of step capacitance. A 0.9 by 0.4 inch waveguide having a step reduction in height corresponding to $\Gamma_r = 0.1$ appears as a pure resistance at a plane 0.37 mm from the step measured along the larger guide. Corresponding values for the other reference reflections are: $\Gamma_r = 0.2$, 0.46 mm, $\Gamma_r = 0.333$, 0.43 mm. As these distances vary only about 1 percent over the frequency band they may be included as a small correction in the computer programs. The programs are also corrected for waveguide attenuation.

## Present Performance and Typical Results

One of the chief advantages of the comparison reflectometer is its ability to locate and measure reflections smaller than those caused by imperfections in the instrument itself. Instrumental reflections contribute both to the reference and measurement sets of readings and ideally should cancel out completely, thus allowing small reflections in the test component to stand out clearly against a quiet background.

As small reflections from the matched load contribute to the reference readings only, at first sight it would appear to be essential to build an almost perfect load in order to measure small reflections. This would be so if both the load and test component were placed at the same distance from the reference plane; but by fitting a length of accurate waveguide in front of the load, the load reflections may be removed from the region being measured. Certainly, reflections from this guide will be superimposed on the output, but it is easier to make an almost reflectionless plain guide

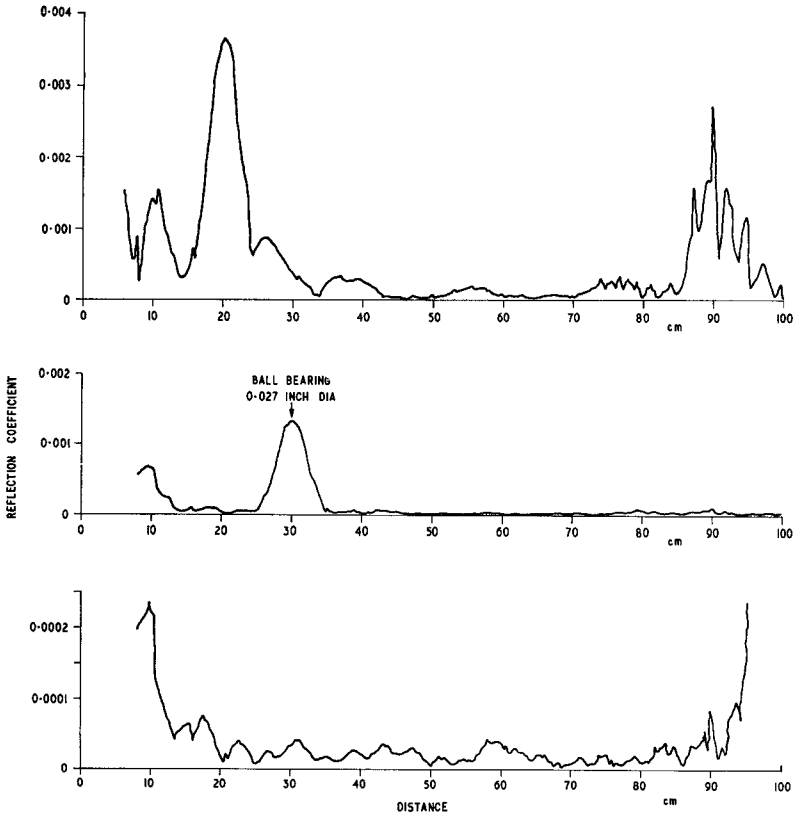


(a) The reflection pattern caused by imperfections in components of the reflectometer, shown before cancellation.

(b) The peaks in (a) have been reduced by the method of cancellation described in the text. The background is now low enough to permit the location and measurement of a small additional reflection, $|\Gamma| = 0.0014$, placed at 30 cm.

(c) The background remaining after cancellation of the instrumental reflections, shown on an expanded scale. Over much of the range $|\Gamma|$ is less than 0.00006.

Fig. 9. The cancellation of instrumental reflections.

than to make a broadband matched load of equal quality.

If any drift in either frequency or amplitude occurs during the period of eight minutes between the two sets of readings, the cancellation of instrumental reflections will be incomplete. Figure 9 shows the results of a test made to examine the effectiveness of this cancellation in practice. Figure 9(a) was obtained by fitting an 89 cm plain guide and load to the reflectometer and computing the reflections by assuming that the value of $E_r$ in (24) remained constant over the whole wavenumber range. Figure 9(a) therefore represents reflections in the instrument and in the plain guide and load. The same plain waveguide was used in Fig. 9(b), but here the instrumental reflections have been cancelled by recording both reference and measurement sets of readings. Between the two sets a 0.027 inch ball bearing[6] was placed near the center of the broad face to test the ability of the instrument to measure and display small reflections.

A more accurate reference waveguide one meter long was then constructed from selected guide. Measurements made with air-bearing, air gauges [4] in three $E$-planes and one $H$-plane showed that the dimensions were uniform within $\pm 0.0001$ inch over the whole length, with the exception of a few centimeters near each flange. The curve shown in Fig. 9(c) was obtained by facing this one-meter guide in one direction during the reference readings and reversing it for the measurement set. The low level of Fig. 9(c) indicates that the cancellation of instrumental reflections is reasonably complete and also that reflections in the plain guide probably do not exceed the level shown, 0.00006.

Figure 10 shows three examples of measurements of microwave components. Figure 10(a) shows reflections in a rotary-vane attenuator and the component parts causing them may be identified in the sectioned diagram below. In these diagrams axial distances have been shown to correct scale but the transverse ($H$-plane) dimensions have been enlarged for clarity. The peaks occurring near the ends of the instrument are not caused by the flanges but by the transitions to circular waveguide. This is a very early design; similar measurements of a modern rotary-vane attenuator showed much lower reflections.

Figure 10(b) and (c) show two different designs of $X$-band slotted guides for standing-wave impedance measurements. Reflections from the ends of the slot are relatively lower in 10(c) but the probe reflection is higher than in 10(b) even though the probe was withdrawn into its shield. The table of phase angles in the computer print-out shows that the probe appears as a shunt capacitance. Note that the right-hand flange of the slotted section shown in 10(b) is slightly defective.

When reflections have been located and measured in this way it is often possible to reduce them: steps are now being taken to improve two of the instruments shown in Fig. 10.

[6] Silver-plated ball bearings, thinly coated with polystyrene, and held in position by small bar magnets external to the guide, have been found useful for matching out small reflections. They may be adjusted readily in both magnitude and phase and often are superior to slide-screw tuners in having lower losses and because of the absence of unwanted reflections from the ends of the slots.

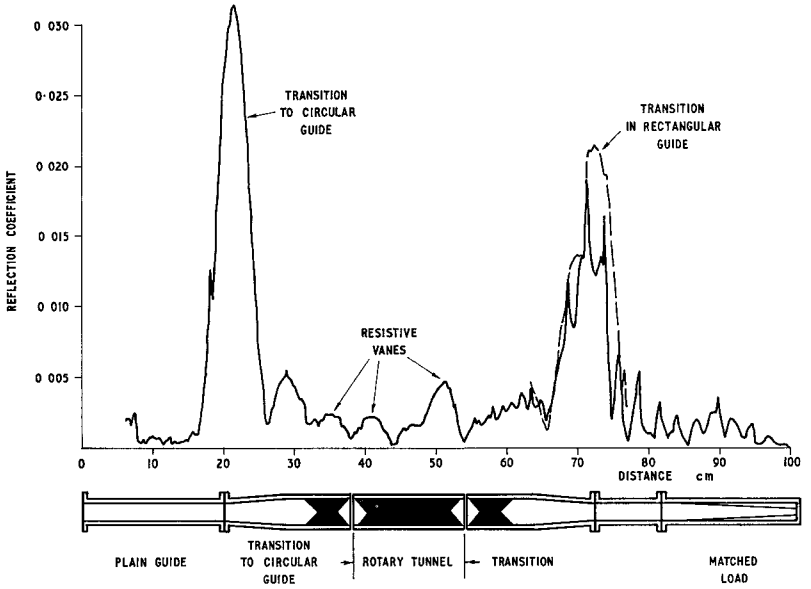


(a) A rotary-vane attenuator set at minimum attenuation. The dotted line shows the shape of the right-hand reflection as measured with the attenuator reversed. The reflections in modern rotary attenuators are much lower than those shown.

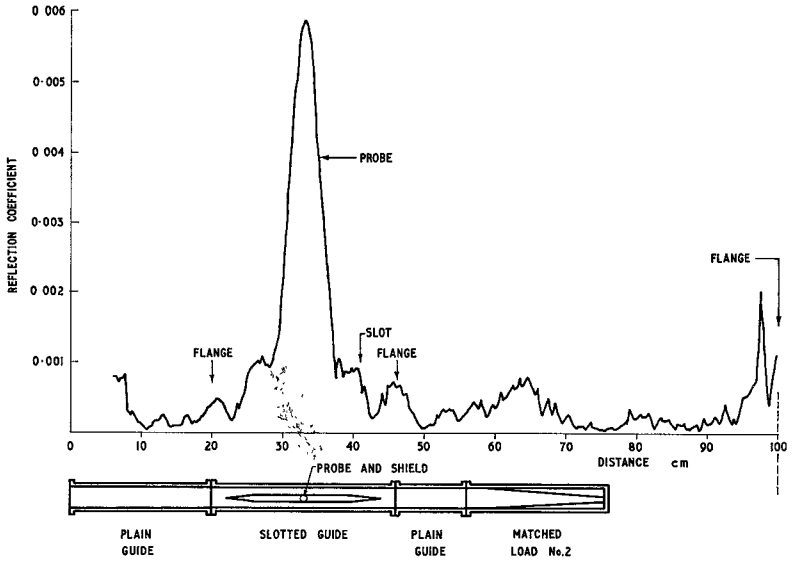


(b) A slotted waveguide for standing-wave impedance measurements. The untuned probe has been withdrawn to give an output of 200 $\mu$V at 3 mW transmitted power and most of the reflection shown is caused by the probe shield.

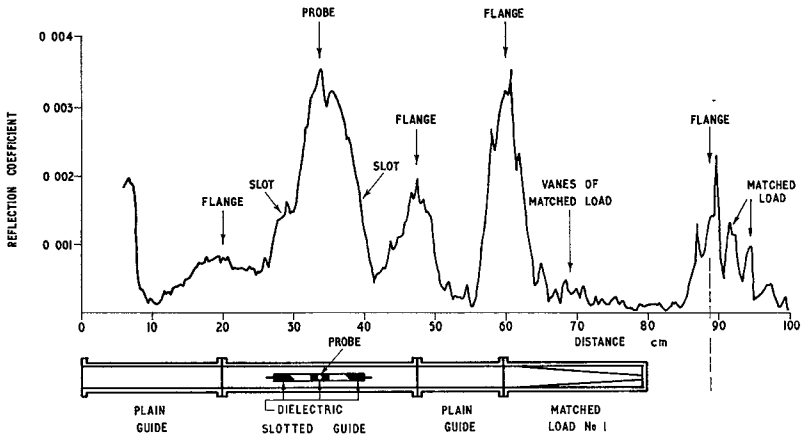


(c) A slotted waveguide of different design. (The peak at 90 cm is contributed by the flange and matched load used in recording the reference set of measurements.)

Fig. 10. Examples of measurements made by the comparison reflectometer to locate unwanted reflections in microwave measuring equipment.

ACKNOWLEDGMENT

The author wishes to thank several members of the National Standards Laboratory: I. G. Morgan contributed helpful suggestions; the paper tape punch control and Serializer are general-purpose data recording units designed by G. J. A. Cassidy and J. Duruz; the noncontacting air gauges were originated by J. Field; and much of the equipment was constructed by C. Ella.

REFERENCES

[1] G. F. Engen and R. W. Beatty, "Microwave reflectometer techniques," *IRE Trans. on Microwave Theory and Techniques*, vol. MTT-7, no. 3, pp. 351–355, July 1959.
[2] J. Willis and N. K. Sinha, "Non-uniform transmission lines as impedance transformers," *Proc. IEE (London)*, vol. 103, pt. B, pp. 166–172, March 1956.
[3] N. Marcuvitz, *Waveguide Handbook*. New York: McGraw-Hill, 1951, ch. 5, pp. 307–308.
[4] J. S. Field, private communication.

# Correction

## "Multiple-Idler Parametric Amplifiers"

R. L. Ernst, author of the above paper, which appeared on pp. 9–22 of the January 1967, issue of this TRANSACTIONS, has called the following to the attention of the Editor.

*On page 10:*

In (5), the terms $S_1^*/j\omega_1$ and $S_1^*/j\omega_2$ should have been preceded by minus signs.

*On page 11:*

$Q_1$ should have been positive, and $Q_k$ is valid only for $k$ greater than one.

*On page 13:*

The first term in the equation preceding (17) should have read $2\zeta_2\omega_s\omega_p^2$.

The derivation for noise temperature in (20) assumes $S_1$ is real; i.e., $S_1 = S_1^* = |S_1|$. This can be done by choosing the angle of pumping properly.

*On page 14:*

Equation (22) should have read

$$\omega_p = \frac{1}{2}\frac{\sqrt{\omega_s^2 + m_1^2\omega_c^2}}{\zeta_1} + \frac{(3\zeta_1 - 2)}{4\zeta_1}\omega_s + \frac{1}{4\zeta_1}\sqrt{[2\sqrt{\omega_s^2 + m_1^2\omega_c^2} + (\zeta_1 - 2)\omega_s]^2 - 8\frac{\zeta_1}{\zeta_2}m_1^2\omega_c^2}.$$

In the equation following (23), the term

$$\zeta_1\left(\frac{m_1\omega_c}{\omega_1} - \frac{m_1\omega_c}{\omega_2}\right)\left[\frac{m_1^3\omega_c^3}{\omega_s^2\omega_1} + \frac{m_1^3\omega_c^3}{\omega_s\omega_1\omega_2} + \zeta_1\left(\frac{m_1\omega_c}{\omega_1} - \frac{m_1\omega_c}{\omega_2}\right)\right]$$

should have been raised to the $\frac{1}{2}$ power.

*On page 17:*

In the equation for noise temperature, the denominator should have been multiplied by $R_s$.

*On page 21:*

The first equality of (61) should have read

$$b_{33} = a_{33} - \frac{a_{34}}{b_{44}}a_{43}.$$

Equation (65) should be identical to (8).